Effects of Hydrogen Addition on the Laminar Flame Speed and Markstein Length of Premixed Dimethyl Ether–Air Flames

ARTICLE *in* ENERGY & FUELS · JULY 2015

Impact Factor: 2.79 · DOI: 10.1021/acs.energyfuels.5b00501

6 AUTHORS, INCLUDING:

Erjiang Hu

Xi'an Jiaotong University

64 PUBLICATIONS **724** CITATIONS

SEE PROFILE

Ke Yang

Xi'an Jiaotong University

5 PUBLICATIONS **4** CITATIONS

SEE PROFILE

Zuohua Huang

Xi'an Jiaotong University

421 PUBLICATIONS **5,195** CITATIONS

SEE PROFILE

energy&fuels

Article

pubs.acs.org/EF

Effects of Hydrogen Addition on the Laminar Flame Speed and Markstein Length of Premixed Dimethyl Ether−Air Flames

Huibin Yu, Erjiang Hu,* Yu Cheng, Ke Yang, Xinyi Zhang, and Zuohua Huang*

State Key Laboratory of Multiphase Flow in Power Engineering, Xi'an Jiaotong University, Xi'an, Shaanxi 710049, People's Republic of China

ABSTRACT: Laminar flame speeds of premixed dimethyl ether/hydrogen/air flames were measured in a constant volume bomb at different temperatures, equivalence ratios, and hydrogen blending ratios. Results reveal that laminar flame speeds increase with an increased hydrogen blending ratio and initial temperature. The Wang model and Zhao model both perform well in predicting laminar flame speeds of the blends. Furthermore, three different models for an effective Lewis number are validated, and the volume-fraction-weighted model performs well in predicting the Markstein length. The effects of hydrogen addition on the flame speed and Markstein length of fuel blends are systematically studied. The chemical kinetic effect induced by hydrogen addition plays a dominant role in increasing the laminar flame speed in comparison to thermal and diffusive effects. In addition, there exists a critical equivalence ratio in the trend of the Markstein length. At the equivalence ratio less than the critical equivalence ratio, the Markstein length decreases with increased hydrogen fraction, indicating that the addition of hydrogen enhances the diffusional thermal instability of the blends. While at the equivalence ratio larger than the critical equivalence ratio, the Markstein length increases with the increase of the hydrogen mole fraction. Finally, the combined parameter $[Ze(Le-1)]$ can reflect the trend of L_b, which varies with the hydrogen blending ratio.

1. INTRODUCTION

With the development of urbanization and industrialization, the inordinate use of petroleum-based fuels is more and more evident, which is one of the major reasons for environmental problems and oil shortage.[1,2] In recent years, these issues have driven researchers to pay attention to alternative fuels as well as more efficient combustion technologies for internal combustion (IC) engines.[3,4]

As a candidate of alternative fuels, dimethyl ether (DME) is one of the promising fuels for IC engines and gas turbines because of its excellent physical and chemical characteristics.[5−8] DME has no carbon−carbon bond and high oxygen content, making it have a lower soot emission.[9] Meanwhile, lean combustion is an advanced technology to obtain higher thermal efficiency as well as lower emission. Nevertheless, lean combustion operation encounters high cycle-to-cycle variations.[10] One method to control cyclic variations is to introduce clean, abundant, and economical gaseous fuels. Ceviz and Yüksel[11] investigated the effect of liquefied petroleum gas (LPG) on the cyclic variations and pollutant emissions in a lean-burn gasoline engine. They revealed that LPG can decrease the coefficient of variations and emissions. Besides, lean hydrocarbon−air mixtures are difficult to ignite and easy to extinguish.[12] Hydrogen has strong chemical reactivity and wide flammability range; therefore, hydrogen addition can increase the combustion intensity and extend the flammability limits of lean mixtures. Besides, hydrogen is also a clean alternative fuel with no carbon emissions.[13] Hence, the use of DME/H_2 blends in lean combustion conditions has the potential to increase the thermal efficiency and reduce pollutant emissions.

The fundamental combustion parameters, such as the laminar flame speed, can characterize the effects of hydrogen addition quantitatively.[14] Thus far, there are a few fundamental combustion studies on DME/hydrogen blends. On the basis of the DME jet diffusion flame, Kang et al.[15] investigated the effects of hydrogen addition on flame structures, flame entrainment, and pollutant emissions over wide hydrogen blending ratios (0−100%). Liu et al.[16,17] numerically studied the effects of hydrogen addition on the intermediate species of premixed DME−oxygen−argon flames and the chemical effect of hydrogen addition, respectively. Huang et al.[18] experimentally studied the laminar flame speeds of DME/H_2/air mixtures at three equivalence ratios (0.8, 1.0, and 1.2) and normal temperature and pressure. Chen et al.[19] studied the effects of hydrogen addition on mole fractions of major intermediates and main products of premixed fuel-rich (ϕ = 1.5) DME/H_2/O_2/Ar flames using molecular beam sampling mass spectrometry techniques and tunable synchrotron vacuum ultraviolet photoionization.

The laminar flame speed is an important parameter for developing and validating the chemical kinetic mechanism. Meanwhile, it embodies the physicochemical properties of flammable gas and is also the fundamental parameter in turbulent combustion modeling. Thus far, little data on laminar flame speeds of DME/H_2/air mixtures are reported, and the effects of H_2 addition on premixed DME/air flame are still not well understood. In this study, laminar flame speeds and Markstein lengths of premixed DME/H_2/air mixtures were measured in a constant volume chamber at a wide range of equivalence ratios (0.7−1.6), hydrogen blending ratios (0, 40, 60, and 80%), and temperatures (303−493 K). More details can be found in Table 1. Moreover, the updated Zhao model[20] by Wang et al.,[21] named as the "Wang model", and the Zhao

Received: March 9, 2015
Revised: June 10, 2015
Published: June 12, 2015

DOI: 10.1021/acs.energyfuels.5b00501
Energy Fuels 2015, 29, 4567−4575

Table 1. Experimental Conditions

P (MPa)	T (K)	X_{H_2} (%)	ϕ
0.1	303	0, 40, 60, and 80	0.7−1.6
0.1	353 and 393	40 and 60	0.7−1.6

model[20] are validated by the experimental data. The Wang model was constructed by updating rate constants of some important DME oxidation reactions at low temperatures. The effect of this update on the laminar flame speed is also examined for the first time. Besides, we validate the three different models for calculating an effective Lewis number proposed by Law et al.,[22] Muppala et al.,[23] and Dinkelacker et al.,[24] respectively. Finally, the effects of hydrogen addition on the laminar flame characteristics of premixed DME/air flame are systematically analyzed.

2. EXPERIMENTAL AND NUMERICAL SPECIFICATIONS

The experimental setup was reported in the previous research.[25,26] Here, a brief description is given. The constant volume chamber is cylindrical, with an inner diameter of 180 mm. A thermocouple and pressure transmitter were used to measure the temperature and pressure, respectively. The initial temperature was maintained with an uncertainty of ±2 K. The elevated temperature was achieved by a heating tap uniformly wrapped around the chamber. Each composition of mixtures was introduced into the chamber according to their partial pressure. The mixtures was ignited by a spark formed at the center of this chamber. Before ignition, the mixture was kept at least 5 min to eliminate the effects of incomplete mixing and gas motion. The spherical flames were recorded by a Phantom high-speed camera operating at 10 000 frames/s. The flame front radius was obtained from flame image post-processing, after background subtraction and a robust regression method. Each condition was repeated at least 3 times. To obtain the laminar flame speed, the stretch effect on the flame propagation speed needs to be removed. The conventional method is the linear extrapolation.[27,28] In 2009, Kelley and Law[29] recommended a nonlinear extrapolation method for the spherically expanding flame to ensure the data accuracy. This nonlinear extrapolation method is also widely used by other research teams, such as Dayma et al.,[30] Galmiche et al.,[31] Ravi et al.,[32] etc.; the references cited here are just representative of the many studies that have published.

The equation is as follows:

$$(S_b/S_b^0)^2 \ln(S_b/S_b^0)^2 = -2L_b\kappa/S_b^0 \quad (1)$$

where S_b and S_b^0 are the stretched and unstretched flame propagation speeds. L_b is the Markstein length. S_b was calculated from the original flame radius (r_f) via

$$S_b = dr_f/dt \quad (2)$$

The flame stretch rate, κ, was derived via

$$\kappa = \frac{1}{A}\frac{dA}{dt} = 2S_b/r_f \quad (3)$$

The laminar flame speed, S_u^0, was determined through

$$S_u^0 = S_b^0\rho_b/\rho_u \quad (4)$$

where ρ_b and ρ_u are the burned and unburned gas densities, respectively. The hydrogen blending ratio (X_{H_2}) is defined as

$$X_{H_2} = \frac{V_{H_2}}{V_{DME} + V_{H_2}} \times 100\% \quad (5)$$

where V_{H_2} and V_{DME} represent the volume fraction of H_2 and DME. Against the traditional definition of the equivalence ratio and hydrogen blending ratio, Yu et al.[12] proposed a different definition of an effective blended fuel−air equivalence ratio (ϕ_F) and hydrogen blending ratio (R_H). ϕ_F and R_H were defined as follows:

$$\phi_F = \frac{C_F/[C_A - C_H/(C_H/C_A)_{st}]}{(C_F/C_A)_{st}} \quad (6)$$

$$R_H = \frac{C_H + C_H/(C_H/C_A)_{st}}{C_F + [C_A - C_H/(C_H/C_A)_{st}]} \quad (7)$$

where C_A, C_H, and C_F are the mole fractions of air, hydrogen, and base fuel (DME), respectively, with $C_A + C_H + C_F = 1$. The subscript st represents the stoichiometric condition. This definition was also adopted by Tang et al.[14] and Hui et al.[33] Their study demonstrated that the laminar flame speeds increase almost linearly with R_H in the range of 0−0.5. In this study, the two different definitions of ϕ_F and R_H are compared and R_H is extended to 1.0.

To remove effects of ignition energy and pressure rise, the radius between 8 and 25 mm was adopted to determine the laminar flame speed.[28,34] Laminar flame speeds were also calculated using the CHEMKIN and PREMIX codes.[35,36] The adiabatic flame temperature and the density of the burned mixture were calculated using the CHEMKIN equilibrium code. In this study, the Zhao model[20] and Wang model[21] were used in the simulation. The final adaptive grid parameters (GRAD and CURV) were both set at 0.02, and more than 800 mesh points were obtained in final solutions. The mixture-averaged transport properties and thermal diffusion (Sort effect) were also considered in calculations.

3. MODEL VALIDATION AND EXPERIMENTAL RESULTS

3.1. Model Validation. Figure 1 gives the measured and calculated laminar flame speeds of premixed DME/air flames.

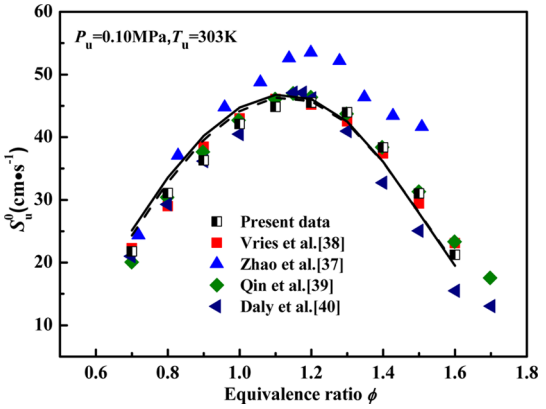

Figure 1. Laminar flame speeds of DME/air flames (symbols, experimental data; solid line, Zhao model; and dashed line, Wang model).

The comparison to previous results by Zhao et al.,[37] Vries et al.,[38] Qin et al.,[39] and Daly et al.[40] is also presented. For DME/air premixed mixtures, present data agree fairly well with the published data, except those by Zhao et al.[37] Data by Zhao et al.[37] are much higher than other data, especially at rich conditions. Good agreement with the calculated results of the Zhao model[20] and Wang model[21] is also presented.

3.2. Laminar Flame Speeds of DME/H_2 Blends. Laminar flame speeds of DME/H_2 blends at 303 K are plotted in Figure 2. The comparison to the Wang model and Zhao model is also presented. As shown in Figure 2, laminar flame speeds of DME/H_2/air mixtures increase with the increase of the hydrogen fraction. On the whole, simulations of both models agree well with the experimental data. Meanwhile, calculated

DOI: 10.1021/acs.energyfuels.5b00501
Energy Fuels 2015, 29, 4567−4575

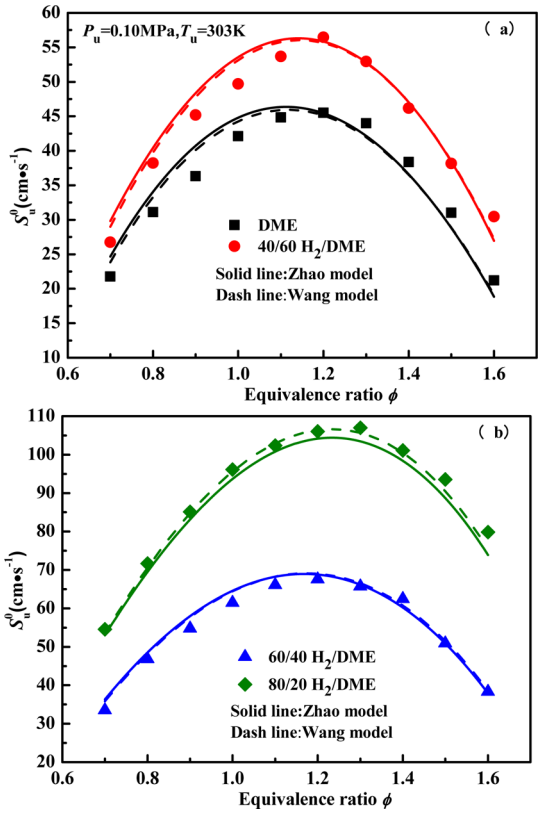

Figure 2. Laminar flame speeds of DME/H_2/air flames (symbols, experimental data; lines, calculated data).

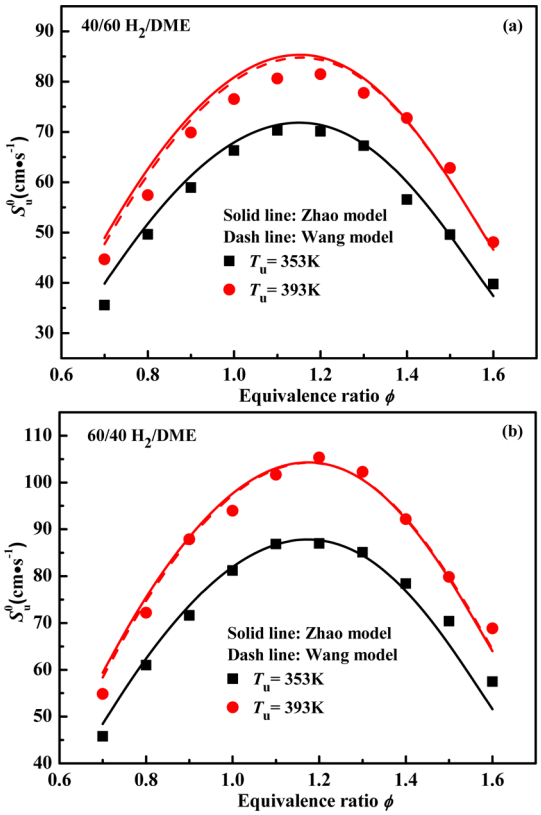

Figure 3. Laminar flame speeds of the 40:60 and 60:40 H_2/DME blends at different initial temperatures.

results of the Wang model and Zhao model are extremely close to each other.

Figure 3 gives laminar flame speeds of the 40:60 and 60:40 H_2/DME mixtures at high initial temperatures. The comparison to the Wang model and Zhao model is also showed. Good agreement with both the Zhao model and Wang model is presented. At high initial temperatures, the Wang model and Zhao model also predict almost the same values. As expected, the laminar flame speeds increase with the increase of the initial temperature. Chain-branching reactions are sensitive to the temperature, and chain-termination reactions are insensitive to the temperature. According to the Arrhenius kinetics, the increase of the initial temperature gives rise to an increase in the adiabatic temperature, which results in the increase of the reaction rate. The increase of the reaction rate promotes the overall reaction progress.

Figure 4 illustrates the measured and calculated laminar flame speeds of the mixtures as a function of the hydrogen fraction (X_{H_2}) and R_H at the temperature of 303 K and pressure of 0.1 MPa. As demonstrated above, the Zhao model and Wang model perform well on the laminar flame speed. Hence, the calculated results using the Zhao model can be used to study the effect of hydrogen addition on the laminar flame speed. It is clear that laminar flame speeds increase nonlinearly with X_{H_2} for all equivalence ratios, while the laminar flame speeds increase almost linearly with R_H over the whole range. In Figure 4a, profiles of the flame speeds are similar to ethanol–hydrogen–air mixtures[41] and can be distinguished by three regimes in terms of X_{H_2}. For $0 < X_{H_2} < 50$, the flame propagation is dominated by properties of DME and the laminar flame speed increases slightly and almost linearly. For $50 < X_{H_2} < 90$, a

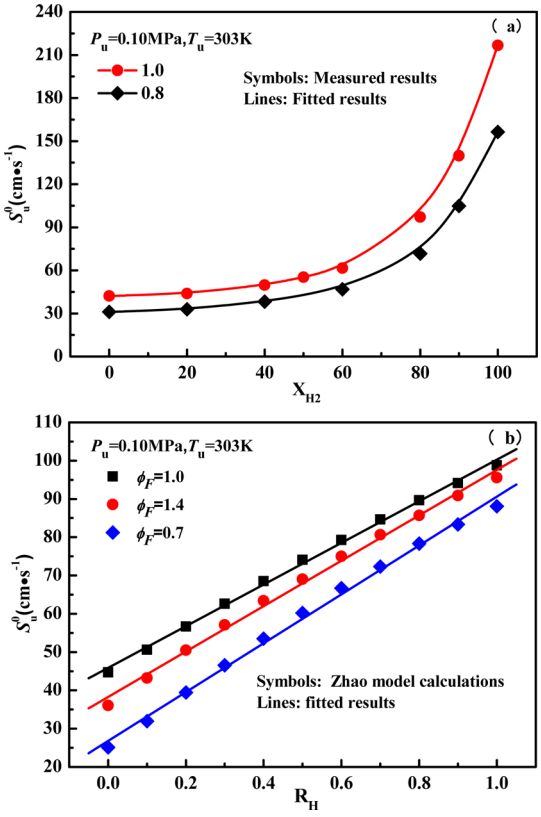

Figure 4. Measured and simulated laminar flame speeds of DME/H_2/air flames as a function of the hydrogen addition ratio and R_H.

DOI: 10.1021/acs.energyfuels.5b00501
Energy Fuels 2015, 29, 4567–4575

transition regime is presented and characterized by an exponential increase of the laminar flame speed. At a high hydrogen blending ratio ($90 < X_{H_2} < 100$), the laminar flame speed increases sharply and almost linearly with an increased hydrogen fraction.

3.3. Markstein Length. Markstein length reflects the sensitivity of flame propagation to the stretch rate and also characterizes the flame instability. Figure 5 shows the Markstein length of the DME/H_2 blends at the temperature of 303 K and pressure of 0.1 MPa. The Markstein length obtained by Tang et al.[42] using a linear extrapolation method is also plotted in Figure 5. The Markstein length of DME/air mixtures decreases with an increased equivalence ratio. It can be seen that there is an inverse variation of the Markstein length between those of DME/air mixtures and hydrogen/air mixtures. There exists a critical equivalence ratio ϕ^* in the trend of the Markstein length. The critical equivalence ratio ϕ^* locates at the region between the equivalence ratio of 1.3 and 1.5. At the equivalence ratio less than ϕ^*, the Markstein length decreased with an increased hydrogen fraction, indicating that the addition of hydrogen enhances the diffusional thermal instability of the blends. While at the equivalence ratio larger than ϕ^*, the Markstein length increased with the increase of the hydrogen mole fraction. Besides, at low hydrogen blending ratios, the trends are similar to that of pure DME, while the trends are similar to that of pure of hydrogen at high hydrogen blending ratios. Therefore, the effect of DME plays a dominant role in flame instability of DME/H_2 mixtures at low hydrogen blending ratios. On the contrary, the properties of hydrogen play a dominant role at high hydrogen blending ratios.

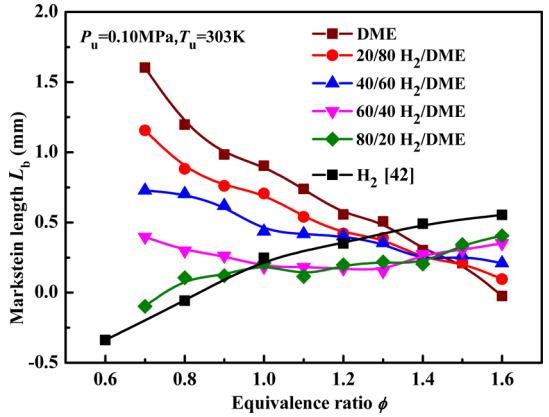

Figure 5. Markstein length of DME/H_2/air flames at different hydrogen blending ratios.

4. DISCUSSION

4.1. Laminar Flame Speed. The effects of hydrogen addition on the laminar flame speed of the DME/air mixture can be classified into diffusive, thermal, and kinetic effects.[14,43] It is of interest to find out which is dominant. In terms of constant transport properties and one-step overall reaction assumption, the laminar flame speed can be correlated with the adiabatic flame temperature (T_{ad}), Lewis number (Le), and activation temperature (T_a)

$$S_u^0 \sim (\alpha Le)^{1/2} \exp(-T_a/2T_{ad}) \quad (8)$$

in which α is the thermal diffusivity. In eq 8, the first term $(\alpha Le)^{1/2}$ represents the diffusion effect. The activation temperature ($T_a = E_a/R$, where E_a and R are the global activation energy and universal gas constant, respectively) represents the kinetic effect. The T_{ad} represents the thermal effect. The second exponential term can be treated as the Arrhenius factor effect, which represents the combined effect of thermal and kinetic effects.

The activation energy can be calculated through the following equation suggested by Law:[44]

$$E_a = -2R[\partial(\ln \rho_u S_u^0)/\partial(1/T_{ad})]_p \quad (9)$$

As discussed in section 4.3, the volume-fraction-weighted model (Le_v) performs well in simulating the Markstein length. Here, Le_v is adopted in eq 8.

Figure 6 depicts the adiabatic flame temperature of DME/H_2 blends at the temperature of 303 K and pressure of 0.1 MPa.

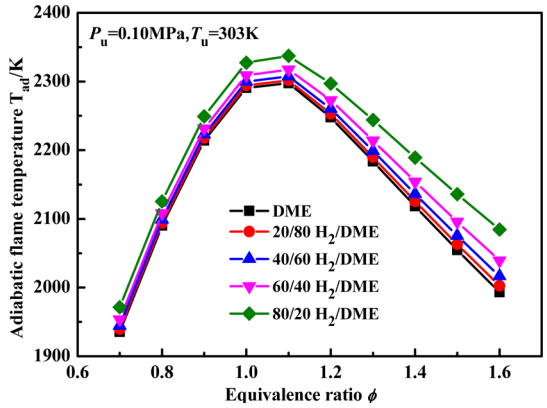

Figure 6. Adiabatic flame temperatures of different mixture at different hydrogen fractions.

The adiabatic flame temperature increases with the increase of the hydrogen blending ratio. To determine which effect is dominant in increasing the laminar flame speed, we need new mixtures that were formed by adding excess nitrogen to obtain the same adiabatic flame temperature with pure DME. The laminar flame speed of nitrogen-rich mixtures was calculated at the same range of equivalence ratios and hydrogen blending ratios. Figure 7 gives the calculated laminar flame speeds of the DME/H_2 blends at the temperature of 303 K and pressure of

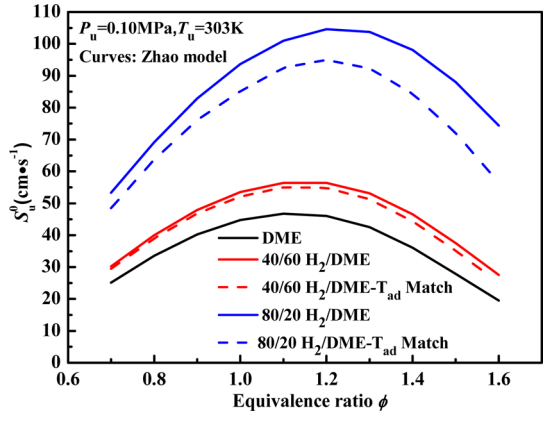

Figure 7. Calculated laminar flame speeds of the 40:60 and 80:20 H_2/DME blends.

DOI: 10.1021/acs.energyfuels.5b00501
Energy Fuels 2015, 29, 4567−4575

0.1 MPa. It can be seen that the laminar flame speeds of nitrogen-rich binary fuel mixtures are lower than those of undiluted binary fuel mixtures. Meanwhile, the laminar flame speeds of nitrogen-rich mixtures are still higher than those of pure DME/air flames. Hence, the increased temperature (thermal effect) does not play an important role in enhancing the laminar flame speeds in comparison to diffusion and kinetic effects.

Figure 8 shows the variations of Arrhenius and diffusion factors for DME/H_2 blends at different hydrogen fractions and

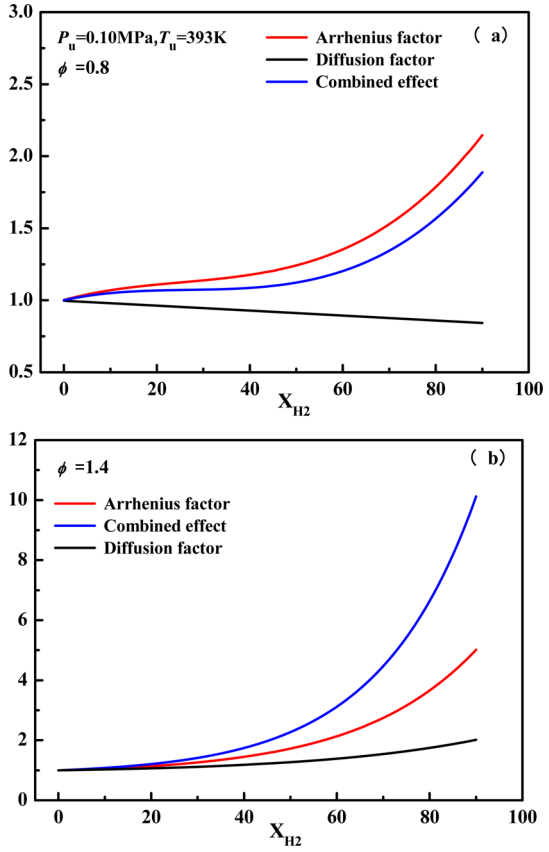

Figure 8. Diffusive and Arrhenius factor effects of H_2 addition on DME for (a) ϕ = 0.8 and (b) ϕ = 1.4. All of the factors are normalized by those of pure DME.

two equivalence ratios. The factors are all normalized by those of pure DME (superscripted by "o"). The Arrhenius factor $[\exp(-T_a/2T_{ad})/\exp(-T_a^o/2T_{ad}^o)]$ invariably plays a positive and dominant role for both lean and rich mixtures when compared to the diffusive factor $[(\alpha Le)^{1/2}/(\alpha^o Le^o)^{1/2}]$. Moreover, the diffusion factor has a negative (positive) effect on the combustion process for lean (rich) conditions. As discussed above, the thermal effect is less important than diffusion and kinetic effects. Hence, the dominant mechanism for the laminar flame speed enhancement of pure DME with hydrogen addition is the kinetic effect.

4.2. Reaction Path Analysis. The analysis above demonstrates that the chemical kinetic effect of hydrogen addition plays a predominant role in increasing the laminar flame speed. Thus, the detailed analysis (integrated consumption path of species) using the Wang model was conducted to gain further insight into the effects of hydrogen addition on DME oxidation.

The major reaction pathway for DME and 40:60 and 80:40 H_2/DME blends is given in Figure 9 at ϕ = 1.0, T_u = 303 K,

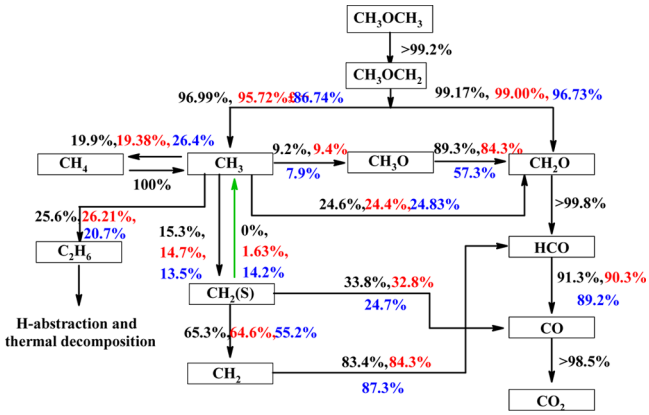

Figure 9. Reaction path analysis of DME and 40:60 and 80:40 H_2/DME blends at ϕ = 1.0, T_u = 303 K, and P_u = 0.1 MPa (black, pure DME; red, 40:60 H_2/DME; and blue, 80:20 H_2/DME).

and P_u = 0.1 MPa. The species around the arrow lines are the main species during the fuel consumption. There are only little differences in the main consumption path with the increase of the hydrogen blending ratio. DME is consumed almost entirely through the H abstraction by free radicals (H, OH, O, and CH_3), forming the methoxymethyl radical (CH_3OCH_2). Decomposition of CH_3OCH_2 through R250 (CH_3OCH_2 = CH_2O + CH_3) is the main consumption path of CH_3OCH_2. Formaldehyde (CH_2O) is then converted almost entirely to formyl radical (HCO), which is converted to CO subsequently. CO is almost entirely converted to CO_2 through R31 (CO + OH = CO_2 + H). At pure DME conditions, the consumption of $CH_2(S)$ through R172 [$CH_2(S)$ + H_2 = CH_3 + H] is not presented. However, this consumption path is becoming obvious with the increase of the hydrogen fraction. In addition, hydrogen is consumed mainly through R2 (O + H_2 = H + OH) and R3 (H_2 + OH = H_2O + H). Figure 10 gives the mole

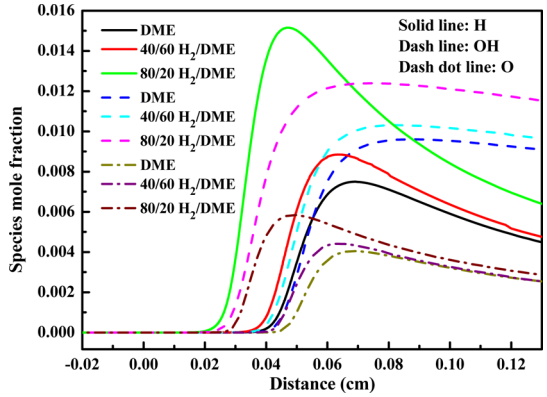

Figure 10. Mole fractions of main species of DME/H_2/air flames at ϕ = 1.0, T_u = 303 K, and P_u = 0.1 MPa.

fractions of major radicals (H, O, and OH) for DME/H_2 blends. It is obvious that the mole fractions of major radicals (H, O, and OH) increase with the increase of the hydrogen blending ratio. The increase of these radicals promote the whole consumption progress, resulting in the increase of the laminar flame speed.

DOI: 10.1021/acs.energyfuels.5b00501
Energy Fuels 2015, 29, 4567−4575

4.3. Markstein Length and Lewis Number. According to the recommendation by Chen et al.,[45,46] L_b can be extracted from the following equation:

$$L_b = [1/Le_{eff} - (Ze/2)(1/Le_{eff} - 1)]\delta_l\sigma \quad (10)$$

where δ_l [$\delta_l = (\lambda/C_p)/(\rho_u S_u^0)$, where C_p is the specific heat and λ is the thermal conductivity calculated using the recommendation by Mathur et al.[47]] is the flame thickness and σ ($\sigma = \rho_u/\rho_b$) is the expansion ratio. The Zeldovich number (Ze) was calculated via

$$Ze = E_a(T_{ad} - T_u)/(RT_{ad}^2) \quad (11)$$

where T_u is the unburned gas temperature.

For single-component fuel at off-stoichiometric conditions, the Lewis number, Le, is defined as the ratio of thermal diffusivity (α) to mass diffusivity of deficient species to the diluent. The effective Lewis number, Le_{eff}, can be calculated through three formulas proposed by Law et al.,[22] Muppala et al.,[23] and Dinkelacker et al.,[24] named as heat release weighted, volume fraction weighted, and mass diffusivity weighted, respectively. More details can be found in Table 2. Because the Markstein length has strong correlation with the Lewis number, it can be used to examine the performance of the three models by calculating the Lewis number.

Table 2. Effective Lewis Number Model[a]

heat release weighted	$Le_H = 1 + \dfrac{q_{H_2}(Le_{H_2} - 1) + q_{DME}(Le_{DME} - 1)}{q_{H_2} + q_{DME}}$
volume fraction weighted	$Le_V = X_{H_2}Le_{H_2} + X_{DME}Le_{DME}$
mass diffusivity weighted	$Le_D = \alpha/(X_{H_2}D_{H_2/N_2} + X_{DME}D_{DME/N_2})$

[a] q_i, non-dimensional heat release; X_i, fuel mole fraction; and D_{i/N_2}, mass diffusivity of deficient species "i" into the diluent.

Figure 11 gives the calculated effective Lewis numbers using the three models for DME/H_2 blends at ϕ = 0.8. The

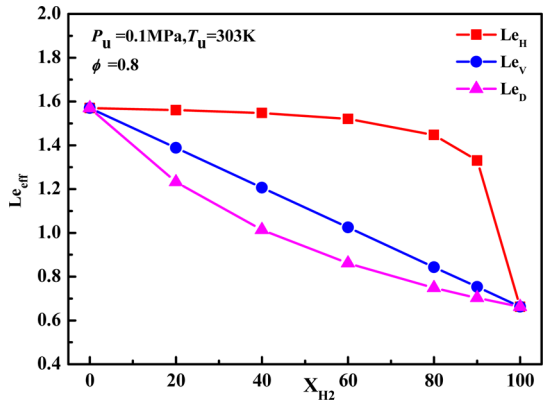

Figure 11. Calculated Lewis number using three models of DME/H_2/air flames at ϕ = 0.8.

remarkable different Lewis numbers are presented for the three Lewis models. Especially for $X_{H_2} > 60$, the volume fraction weighted is greater than 1.0, while mass diffusivity weighted is less than 1.0. This can result in the opposite flame instability analysis according to the flame dynamics theory.[48] The calculated values using the heat-release-weighted model are much higher than the other two models. The heat-release-weighted formula is a weighted average of the Lewis number of the two fuels based on their representative non-dimensional heat release. In calculation, it is actually weighted by their mass fraction. Although the volume fraction of hydrogen is large, the mass fraction is actually small. This may cause the large difference with the other formulas. The volume-fraction-weighted and the mass-diffusivity-weighted formulas are proposed using a similar method. The difference between volume-fraction-weighted and mass-diffusivity-weighted formulas is caused by the different weighted parameters. Therefore, it is necessary to further examine the three models.

Figure 12 shows the experimental and numerical Markstein length of DME/H_2/air mixtures at lean conditions (ϕ = 0.8).

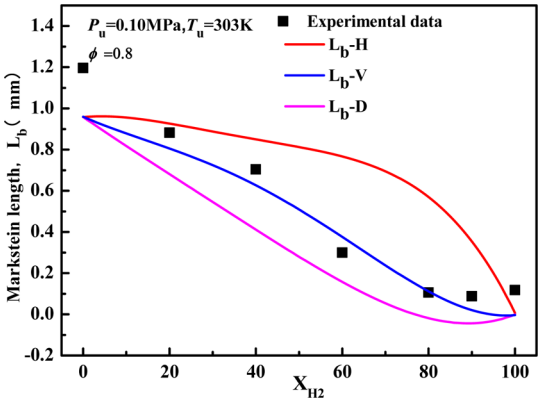

Figure 12. Experimental and numerical Markstein length of DME/H_2/air flames at ϕ = 0.8.

Moreover, results of the calculated Markstein length using the three Lewis number models are also compared to experimental data. The mass-diffusivity-weighted and volume-fraction-weighted models perform well in predicting the variation of L_b while the heat release-weighted model presents the large scatters. With regard to the mass-diffusivity-weighted and volume-fraction-weighted models, the latter performs better. In comparison of Figures 11 and 12, it is clear that the effective Lewis number does not reflect the trend of L_b accurately, especially at high hydrogen blending ratios. It is of interest to investigate which parameter actually controls the trend of L_b.

According the analysis of Law and Sung[48] and Clavin and Williams,[49] the L_b has proportional correlation with the Lewis number, flame thickness, density ratio, and Zeldovich number, namely, $L_b \sim Ze(Le - 1)\sigma\delta$. Figure 13 illustrates the parameters (effective Lewis number, density ratio, flame thickness, and Zeldovich number) that affect the Markstein length as a function of the hydrogen fraction at ϕ = 0.8. From Figure 13a, it can be seen that the Zeldovich number decreases with the increase of the hydrogen blending ratio. This indicates that the global active energy decreases with the increase of the hydrogen mole fraction. According to a one-step reaction mechanism, the combustion process is promoted and then laminar flame speeds increase. From Figure 13, it is clear that the single parameter deceases monotonously with the increase of the hydrogen blending ratio and fails to reflect the trend of L_b at a high hydrogen fraction, while the combined parameter $[Ze(Le - 1)]$ can reflect the whole trend accurately.

DOI: 10.1021/acs.energyfuels.5b00501
Energy Fuels 2015, 29, 4567−4575

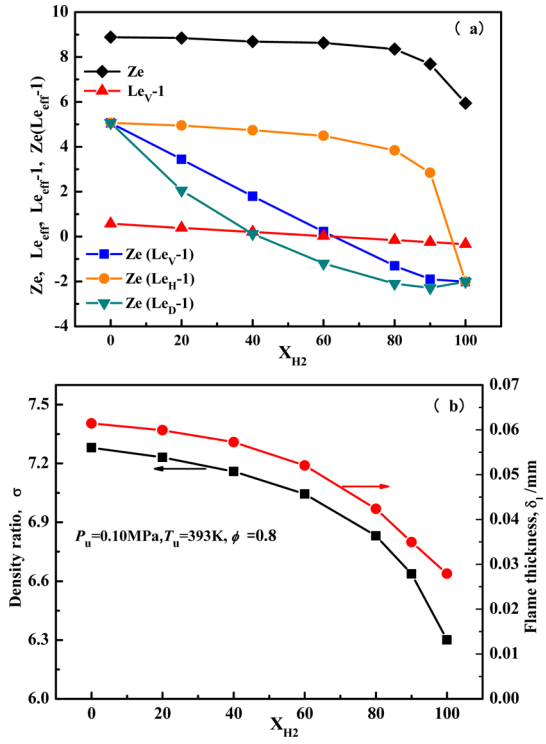

Figure 13. Effects of hydrogen addition on the Lewis number, density ratio, flame thickness, and Zeldovich number.

5. CONCLUSION

Laminar flame speeds of premixed DME/H_2/air flames were measured in a constant volume bomb over a wide range of equivalence ratios and hydrogen blending ratios. The effects of hydrogen addition on laminar flame characteristics of DME/hydrogen/air flames were also studied. Kinetic analysis was performed using the Wang model and Zhao model. Main conclusions are as follows: (1) Laminar flame speeds increase with the increase of the hydrogen blending ratio and initial temperature. In addition, the Wang model and Zhao model both perform well in predicting laminar flame speeds of DME/H_2/air mixtures. (2) The thermal effect is less important than diffusive and kinetic effects. Besides, the dominant mechanism of hydrogen addition on the laminar flame speed is the kinetic effect. There are not large differences in the main consumption path with the increase of the hydrogen blending ratio. The consumption of $CH_2(S)$ through R172 [$CH_2(S) + H_2 = CH_3 + H$] is becoming obvious with the increase of the hydrogen fraction, while this consumption path is not presented at pure DME conditions. (3) There exists a critical equivalence ratio ϕ^* in the trend of the Markstein length. At the equivalence ratio less than ϕ^*, the Markstein length decreases with an increased hydrogen fraction, indicating that the addition of hydrogen enhances the diffusional thermal instability of the blends. While at the equivalence ratio larger than ϕ^*, the Markstein length increases with the increase of the hydrogen mole fraction. (4) The volume-fraction-weighted Lewis number model performs better in predicting the L_b than heat-release-weighted and mass-diffusivity-weighted models, and the combined parameter $[Ze(Le - 1)]$ can reflect the whole trend of L_b accurately.

AUTHOR INFORMATION

Corresponding Authors

*Telephone: 86-29-82665075. Fax: 86-29-82668789. E-mail: hujiang@mail.xjtu.edu.cn.

*Telephone: 86-29-82665075. Fax: 86-29-82668789. E-mail: zhhuang@mail.xjtu.edu.cn.

Notes

The authors declare no competing financial interest.

ACKNOWLEDGMENTS

This work is supported by the National Natural Science Foundation of China (51306144 and 91441118) and the National Basic Research Program (2013CB228406). The authors also appreciate the funding support from the Fundamental Research Funds for the Central Universities.

NOMENCLATURE

r_f = original flame radius (cm)
ϕ = equivalence ratio
P_u = initial pressure (MPa)
T_u = initial temperature (K)
κ = stretch rate (s^{-1})
S_b = stretched flame propagation speed (cm s^{-1})
S_u^0 = laminar flame speed (cm s^{-1})
S_b^0 = unstretched flame propagation speed (cm s^{-1})
ρ_u = density of unburned gas mixtures (kg m^{-3})
ρ_b = density of burned gas mixtures (kg m^{-3})
V_{H_2} = volume fraction of H_2
V_{DME} = volume fraction of DME
ϕ_F = effective blended fuel−air equivalence ratio
R_H = effective hydrogen blending ratio
C_A = mole fraction of air
C_H = mole fraction of hydrogen
C_F = mole fraction of base fuel (DME)
X_{H_2} = hydrogen blending ratio
T_a = activation temperature (K)
T_{ad} = adiabatic temperature (K)
L_b = Markstein length (mm)
δ_l = laminar flame thickness (mm)
σ = density ratio
E_a = global activation energy (kJ/mol)
R = universal gas constant (J mol^{-1} K^{-1})
Ze = Zeldovich number
α = thermal diffusivity (m^2/s)
Le = Lewis number
Le_{eff} = effective Lewis number
ϕ^* = critical equivalence ratio

REFERENCES

(1) Salvi, B. L.; Subramanian, K. A.; Panwar, N. L. Alternative fuels for transportation vehicles: A technical review. *Prog. Energy Combust. Sci.* **2013**, *25*, 404−419.

(2) Azizi, Z.; Rezaeimanesh, M.; Tohidian, T.; Rahimpour, M. R. Dimethyl ether: A review of technologies and production challenges. *Chem. Eng. Process.* **2014**, *82*, 150−172.

(3) Okafor, E. C.; Hayakawa, A.; Nagano, Y.; Kitagawa, T. Effects of hydrogen concentration on premixed laminar flames of hydrogen−methane−air. *Int. J. Hydrogen Energy* **2014**, *39* (5), 2409−2417.

(4) Park, O.; Veloo, P. S.; Liu, N.; Egolfopoulos, F. N. Combustion characteristics of alternative gaseous fuels. *Proc. Combust. Inst.* **2011**, *33* (1), 887−894.

(5) Semelsberger, T. A.; Borup, R. L.; Greene, H. L. Dimethyl ether (DME) as an alternative fuel. *J. Power Sources* **2006**, *156* (2), 497−511.

DOI: 10.1021/acs.energyfuels.5b00501
Energy Fuels 2015, 29, 4567−4575

(6) Tang, C.; Wei, L.; Zhang, J.; Man, X.; Huang, Z. Shock tube measurements and kinetic investigation on the ignition delay times of methane/dimethyl ether mixtures. *Energy Fuels* **2012**, *26* (11), 6720−6728.
(7) Wang, Y. L.; Holley, A. T.; Ji, C.; Egolfopoulos, F. N.; Tsotsis, T. T.; Curran, H. J. Propagation and extinction of premixed dimethyl-ether/air flames. *Proc. Combust. Inst.* **2009**, *32* (1), 1035−1042.
(8) Kim, M. Y.; Yoon, S. H.; Park, K. H.; Lee, C. S. Effect of multiple injection strategies on the emission characteristics of dimethyl ether (DME)-fueled compression ignition engine. *Energy Fuels* **2007**, *21* (5), 2673−2681.
(9) Liang, C.; Ji, C.; Gao, B.; Liu, X.; Zhu, Y. Investigation on the performance of a spark-ignited ethanol engine with DME enrichment. *Energy Convers. Manage.* **2012**, *58*, 19−25.
(10) Alagumalai, A. Internal combustion engines: Progress and prospects. *Renewable Sustainable Energy Rev.* **2014**, *38*, 561−571.
(11) Ceviz, M. A.; Yüksel, F. Cyclic variations on LPG and gasoline-fuelled lean burn SI engine. *Renewable Energy* **2006**, *31* (12), 1950−1960.
(12) Yu, G.; Law, C. K.; Wu, C. K. Laminar flame speeds of hydrocarbon + air mixtures with hydrogen addition. *Combust. Flame* **1986**, *63* (3), 339−347.
(13) Verhelst, S.; Wallner, T. Hydrogen-fueled internal combustion engines. *Prog. Energy Combust. Sci.* **2009**, *35* (6), 490−527.
(14) Tang, C. L.; Huang, Z. H.; Law, C. K. Determination, correlation, and mechanistic interpretation of effects of hydrogen addition on laminar flame speeds of hydrocarbon−air mixtures. *Proc. Combust. Inst.* **2011**, *33* (1), 921−928.
(15) Kang, Y.; Lu, X.; Wang, Q.; Gan, L.; Ji, X.; Wang, H.; Guo, Q.; Song, D.; Ji, P. Effect of H_2 addition on combustion characteristics of dimethyl ether jet diffusion flame. *Energy Convers. Manage.* **2015**, *89*, 735−748.
(16) Liu, J.; Wang, H.; Ouyang, M. Kinetic modeling study of hydrogen addition to premixed dimethyl ether−oxygen−argon flames. *Int. J. Hydrogen Energy* **2011**, *36* (24), 15860−15867.
(17) Liu, D. Kinetic analysis of the chemical effects of hydrogen addition on dimethyl ether flames. *Int. J. Hydrogen Energy* **2014**, *39* (24), 13014−13019.
(18) Huang, Z.; Chen, G.; Chen, C.; Miao, H.; Wang, X.; Jiang, D. Experimental study on premixed combustion of dimethyl ether−hydrogen−air mixtures. *Energy Fuels* **2008**, *22* (2), 967−971.
(19) Chen, Z.; Wei, L.; Gu, X.; Huang, Z.; Yuan, T.; Li, Y.; Tian, Z. Study of low-pressure premixed dimethyl ether/hydrogen/oxygen/argon laminar flames with photoionization mass spectrometry. *Energy Fuels* **2010**, *24* (3), 1628−1635.
(20) Zhao, Z.; Chaos, M.; Kazakov, A.; Dryer, F. L. Thermal decomposition reaction and a comprehensive kinetic model of dimethyl ether. *Int. J. Chem. Kinet.* **2008**, *40* (1), 1−18.
(21) Wang, Z.; Zhang, X.; Xing, L.; Zhang, L.; Herrmann, F.; Moshammer, K.; Qi, F.; Kohse-Höinghaus, K. Experimental and kinetic modeling study of the low- and intermediate-temperature oxidation of dimethyl ether. *Combust. Flame* **2015**, *162* (4), 1113−1125.
(22) Law, C. K.; Jomaas, G.; Bechtold, J. K. Cellular instabilities of expanding hydrogen/propane spherical flames at elevated pressures: Theory and experiment. *Proc. Combust. Inst.* **2005**, *30* (1), 159−167.
(23) Muppala, S. P. R.; Nakahara, M.; Aluri, N. K.; Kido, H.; Wen, J. X.; Papalexandris, M. V. Experimental and analytical investigation of the turbulent burning velocity of two-component fuel mixtures of hydrogen, methane and propane. *Int. J. Hydrogen Energy* **2009**, *34* (22), 9258−9265.
(24) Dinkelacker, F.; Manickam, B.; Muppala, S. P. R. Modelling and simulation of lean premixed turbulent methane/hydrogen/air flames with an effective Lewis number approach. *Combust. Flame* **2011**, *158* (9), 1742−1749.
(25) Hu, E.; He, J.; Huang, Z.; Jin, C.; Miao, H.; Wang, X. Measurements of laminar burning velocities and flame stability analysis for hydrogen−air−diluent mixtures. *Chin. Sci. Bull.* **2009**, *54* (5), 846−857.
(26) Hu, E.; Fu, J.; Pan, L.; Jiang, X.; Huang, Z.; Zhang, Y. Experimental and numerical study on the effect of composition on laminar burning velocities of $H_2/CO/N_2/CO_2$/air mixtures. *Int. J. Hydrogen Energy* **2012**, *37* (23), 18509−18519.
(27) Dowdy, D. R.; Smith, D. B.; Taylor, S. C.; Williams, A. The use of expanding spherical flames to determine burning velocities and stretch effects in hydrogen/air mixtures. *Symp. (Int.) Combust.* **1991**, *23* (1), 325−332.
(28) Bradley, D.; Gaskell, P. H.; Gu, X. J. Burning velocities, markstein lengths, and flame quenching for spherical methane-air flames: A computational study. *Combust. Flame* **1996**, *104* (1−2), 176−198.
(29) Kelley, A. P.; Law, C. K. Nonlinear effects in the extraction of laminar flame speeds from expanding spherical flames. *Combust. Flame* **2009**, *156* (9), 1844−1851.
(30) Dayma, G.; Halter, F.; Foucher, F.; Mounaim-Rousselle, C.; Dagaut, P. Laminar burning velocities of C_4−C_7 ethyl esters in a spherical combustion chamber: Experimental and detailed kinetic modeling. *Energy Fuels* **2012**, *26* (11), 6669−6677.
(31) Galmiche, B.; Halter, F.; Foucher, F.; Dagaut, P. Effects of dilution on laminar burning velocity of premixed methane/air flames. *Energy Fuels* **2011**, *25* (3), 948−954.
(32) Ravi, S.; Sikes, T. G.; Morones, A.; Keesee, C. L.; Petersen, E. L. Comparative study on the laminar flame speed enhancement of methane with ethane and ethylene addition. *Proc. Combust. Inst.* **2015**, *35* (1), 679−686.
(33) Hui, X.; Zhang, C.; Xia, M.; Sung, C.-J. Effects of hydrogen addition on combustion characteristics of *n*-decane/air mixtures. *Combust. Flame* **2014**, *161* (9), 2252−2262.
(34) Burke, M. P.; Chen, Z.; Ju, Y.; Dryer, F. L. Effect of cylindrical confinement on the determination of laminar flame speeds using outwardly propagating flames. *Combust. Flame* **2009**, *156* (4), 771−779.
(35) Kee, R. J.; Rupley, F. M.; Miller, J. A. *CHEMKIN-II: A Fortran Chemical Kinetics Package for the Analysis of Gas-Phase Chemical Kinetics*; Sandia National Laboratory: Albuquerque, NM, 1989; SAND Report 89-8009.
(36) Kee, R. J.; Grcar, J. F.; Smooke, M.; Miller, J. *PREMIX: A Fortran Program for Modeling Steady Laminar One-Dimensional Premixed Flames*; Sandia National Laboratory: Albuquerque, NM, 1985; SAND Report 85-8240.
(37) Zhao, Z.; Kazakov, A.; Dryer, F. Measurements of dimethyl ether/air mixture burning velocities by using particle image velocimetry. *Combust. Flame* **2004**, *139* (1), 52−60.
(38) de Vries, J.; Lowry, W. B.; Serinyel, Z.; Curran, H. J.; Petersen, E. L. Laminar flame speed measurements of dimethyl ether in air at pressures up to 10 atm. *Fuel* **2011**, *90* (1), 331−338.
(39) Qin, X.; Ju, Y. Measurements of burning velocities of dimethyl ether and air premixed flames at elevated pressures. *Proc. Combust. Inst.* **2005**, *30* (1), 233−240.
(40) Daly, C. A.; Simmie, J. M.; Würmel, J.; Djebaïli, N.; Paillard, C. Burning velocities of dimethyl ether and air. *Combust. Flame* **2001**, *125* (4), 1329−1340.
(41) Al-Hamamre, Z.; Yamin, J. The effect of hydrogen addition on premixed laminar acetylene−hydrogen−air and ethanol−hydrogen−air flames. *Int. J. Hydrogen Energy* **2013**, *38* (18), 7499−7509.
(42) Tang, C.; Huang, Z.; Jin, C.; He, J.; Wang, J.; Wang, X.; Miao, H. Laminar burning velocities and combustion characteristics of propane−hydrogen−air premixed flames. *Int. J. Hydrogen Energy* **2008**, *33* (18), 4906−4914.
(43) Wu, F.; Kelley, A. P.; Tang, C.; Zhu, D.; Law, C. K. Measurement and correlation of laminar flame speeds of CO and C_2 hydrocarbons with hydrogen addition at atmospheric and elevated pressures. *Int. J. Hydrogen Energy* **2011**, *36* (20), 13171−13180.
(44) Law, C. K. *Combustion Physics*; Cambridge University Press: Cambridge, U.K., 2006.
(45) Chen, Z.; Burke, M.; Ju, Y. Effects of Lewis number and ignition energy on the determination of laminar flame speed using propagating spherical flames. *Proc. Combust. Inst.* **2009**, *32* (1), 1253−1260.

DOI: 10.1021/acs.energyfuels.5b00501
Energy Fuels 2015, 29, 4567−4575

(46) Chen, Z.; Ju, Y. Theoretical analysis of the evolution from ignition kernel to flame ball and planar flame. *Combust. Theory Modell.* **2007**, *11* (3), 427−453.
(47) Mathur, S.; Tondon, P.; Saxena, S. Thermal conductivity of binary, ternary and quaternary mixtures of rare gases. *Mol. Phys.* **1967**, *12* (6), 569−579.
(48) Law, C. K.; Sung, C. J. Structure, aerodynamics, and geometry of premixed flamelets. *Prog. Energy Combust. Sci.* **2000**, *26* (4−6), 459−505.
(49) Clavin, P.; Williams, F. Effects of molecular diffusion and of thermal expansion on the structure and dynamics of premixed flames in turbulent flows of large scale and low intensity. *J. Fluid Mech.* **1982**, *116*, 251−282.

DOI: 10.1021/acs.energyfuels.5b00501
Energy Fuels 2015, 29, 4567−4575